Multispectral camera and radiative transfer equation used to depict Leonardo's sfumato in *Mona Lisa*

Mady Elias[1,2,*] and Pascal Cotte[3]

[1]Institut des NanoSciences de Paris, Université Pierre et Marie Curie, Unité Mixte de Recherche 7588, Centre National de la Recherche Scientifique, Campus Boucicaut, 140 rue de Lourmel, 75 015 Paris, France

[2]Université d'Evry Val d'Essonne, boulevard François Mitterrand, 91000 Evry, France

[3]Lumiere Technology S.A.S., 215 bis Boulevard St. Germain, 75 006 Paris, France

*Corresponding author: elias@physique.univ-evry.fr

Received 8 January 2008; revised 13 March 2008; accepted 14 March 2008; posted 17 March 2008 (Doc. ID 91529); published 0 MONTH 0000

The technique used by Leonardo da Vinci to paint flesh tints—the sfumato—has never been scientifically depicted until now. From 100,000,000 reflectance spectra recorded on *Mona Lisa*, a virtual removal of the varnish is first obtained. A unique umber pigment is then identified in the upper layer and an exceptional maximum of the color saturation is underlined, both characteristics of a glaze technique. The modeling calling upon the radiative transfer equation confirms this maximum of saturation, the identification of an umber in the upper layer, and moreover underlines a mixture of 1% vermilion and 99% lead white in the base layer. Finally, the modeling, using the auxiliary function method, explains the spectacular maximum of saturation by the multiple scattering. © 2008 Optical Society of America

OCIS codes: 300.6550, 110.4234, 030.5620, 290.4210, 330.1690.

1. Introduction

This study is the first direct application of previous theoretical research on art glazes, already published in the same review [1,2], to a real painting. In this artistic technique, the pigments are the only scattering centers. The pigments are randomly spread with a very low volume concentration (∼2%) in a transparent binder (mainly linseed oil). The artist only varies the number of glaze layers to modulate the lightness and the color saturation without adding any white or black pigments, and thus creates a typical exceptional rendering [3]. Previous research has explained this special visual appearance by studying the interaction between light and matter, calling upon the radiative transfer equation (RTE) [4] and using the exact solving of the auxiliary function method (AFM) [5]. A very simple model with an isotropic phase function for each identical pigment, plane interfaces and a Lambertian scattering base layer have been perfectly validated by comparison between the modeling and the bidirectional spectrometric measurements on school samples [1]. Especially the color variations obtained with this technique lead to an exceptional maximum of saturation that no other technique can reach and that can be considered as the specificity of a glaze. This property has been explained by the calculation of the different light flux in the pictorial layer showing the predominance of the multiple scattering, which is magnified by the low concentration of scatterers [2].

Here we intend to implement the inverse process, i.e., to guess if a glaze technique has been used in a real painting and with which components, starting from experimental reflectance spectra. We chose to study the Joconda, painted by Leonardo da Vinci in Florence between 1503 and 1506, for its international importance, but also because the rendering of

0003-6935/08/160001-09$15.00/0

her flesh tint is one of the present crucial subjects of research in art history and Leonardo never wrote any description of his method. A particular word, the "sfumato" (coming from a past participle of the Italian verb "sfumare") has been coined [6] to describe Leonardo's technique, expressing fine shading and soft transitions between colors and tones. Much historical and scientific information can assume a glaze in Leonardo's sfumato [7], a technique devised by the Primitive Flemish painters, when the Italian artists painted the faces at the same time with a mixture of pigments, currently made of vermilion and lead white. Vasari [8] in 1550 explained that the Italian painter Antonello da Messina, after his long Flemish stay, taught the glaze technique to his Italian friends such as Leonardo da Vinci. Several art historians then suggested a micropointillism [9] or a stratification of translucent paint layers [10]. However, most of them focus on the effect produced by the technique [11–14]. With the same aim, numerous scientists have taken part in a better knowledge of the masterpiece, mostly focusing on the understanding of the emotion expressed by *Mona Lisa*'s face [15–18]. Finally, a measurement campaign took place in 2004 using only nondestructive methods in order to explore the used materials and their locations. A high-resolution three-dimensional (3D) scanner using a color coded depth image has underlined a succession of thinly applied layers with different thicknesses in *Mona Lisa*'s face [19]. X-ray fluorescence has identified mercury, lead, iron, and manganese in different locations of the face, certainly due to the presence of vermilion (mercury sulfide), lead white (lead carbonate), and umber (iron oxide with a small quantity of manganese) pigments [20]. Finally, multispectral imaging has been implemented and the recorded spectra are analyzed in this paper.

The huge advantage of a multispectral camera is to simultaneously record 100,000,000 reflectance spectra on the whole painting in a short time. These raw data are analyzed in Section 2. They allow us to provide a virtual unvarnishing of the painting to identify the pigments embedded in the superficial layers, and to calculate the trichromatic coordinates for each spectrum and thus for each location. The modeling is then implemented in Section 3, calling upon RTE and AFM, and using the pigment identified in Subsection 2.C with their optical properties and different assumptions for the base layer. The modeling leads to results in good accordance with the experimental spectra only for a given base layer, which is then identified. Thus Section 3 presents a new nondestructive method to depict the composition of stratified layers and moreover it confirms the use of a glaze technique in *Mona Lisa*'s sfumato. Subsection 3.B explains the exceptional maximum of color saturation of the sfumato by the separation of the different light flux here applied to *Mona Lisa*'s face.

2. *Mona Lisa*'s Reflectance Spectra

A. Multispectral Camera

The high-definition multispectral camera [21] conceived by Lumiere and Technology uses a 12,000 pixel CCD sensor. A stepper motor moves the sensor on 20,000 vertical lines in order to obtain a maximum definition of 240,000,000 pixels on each channel. The recording process uses 13 filters with 40 nm bandpass, 10 filters in the visible range, and 3 filters in the infrared range. The correction process is applied to take into account the focusing on each channel. The lighting is obtained with two elliptic projectors made of eight halogen lamps synchronized with the sensor moving and providing a $100,000$ lx illumination of the 53 cm × 78 cm painting. The nonuniformity and anisotropy of the illumination is corrected by spectrometric measurements of a white board [21]. The obtained configuration is close to 57°/0°, and allows neglecting the light reflected by the upper surface in the collected beams. For each of the 100,000,000 used pixels, 13 reflectance factors are recorded using a white reference for the normalization and smoothed with the pseudoinverse method to get the corresponding diffuse reflectance spectra [22]. Figure 1(a) presents the result of the scanning.

B. *Mona Lisa* Virtually Unvarnished

To analyze the spectra and to depict the composition of the sfumato, the aged varnish present on the painting, and inducing an important yellowing, must necessarily be taken into account.

A first method can calculate the modification of the light scattered by the paint due to the varnish. The latter induces a light absorption according to Beer's law and a multiplicative factor reducing the reflectance factors, which depends on the wavelength [23]. It also induces a leveling of the paint surface involving a downward translation of the spectra [24]. These physical properties depend on the nature of the varnish and on its state of degradation. Unfortunately, no varnish identification has been implemented during the measurement campaign and this method cannot be used here.

So, a second statistical procedure of virtual varnish removal has been used from the reflectance spectra initially recorded. For this purpose a color chart of varnished and unvarnished paints, made of classical pigments used in Italy in the 16th century and different kinds of artificially aged varnishes, has been realized. After comparison of the varnished and unvarnished spectra of the chart, a mean multiplicative factor was deduced for each wavelength and applied to *Mona Lisa*'s spectra [25].

Figure 1(b) presents the results of this virtual varnish removal, showing the possible original colors as they were when Leonardo offered the painting to King François I. In particular the lapis lazuli identified in the sky has lost its green color due to the yellow old varnish and has recovered its blue hue. It is

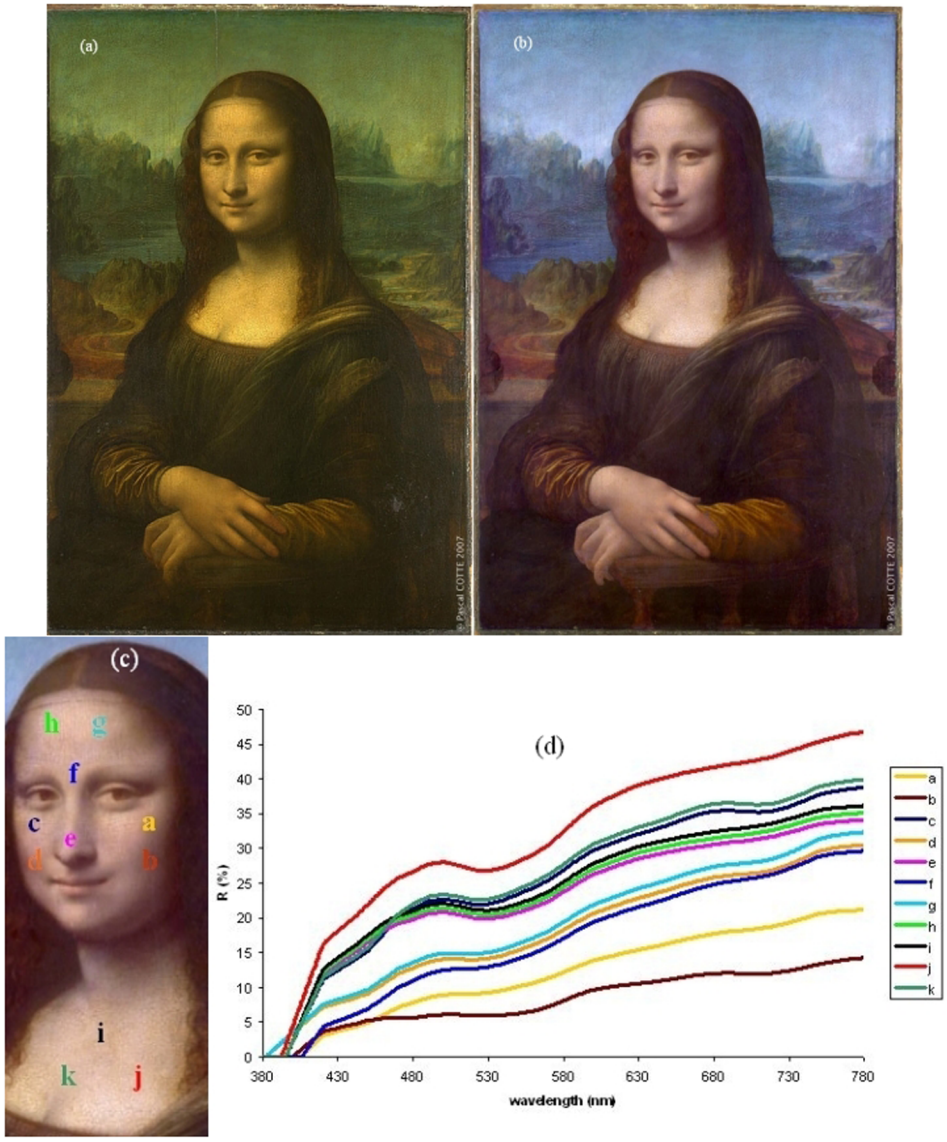

Fig. 1. (Color online) *Mona Lisa* (a) Today, image obtained with the multispectral camera. (b) After virtual removal of the varnish. (c) Eleven selected areas in the unvarnished face. (d) Diffuse reflectance spectra of the 11 locations.

the same for the face that finds again its predominant pink hue.

To study the sfumato, we now focus only on *Mona Lisa*'s face, where about 10,000,000 spectra have been recorded and virtually unvarnished. Only 11 locations have been selected in the face [see Fig. 1(c)], and the corresponding unvarnished spectra are presented [see Fig. 1(d)], allowing a clear discrimination between the spectra. All the other spectra stand between the presented ones and can be deduced one from the other by a vertical translation.

C. Pigment Identification of the Upper Layer

All the spectra show the same characteristics: the slope breaks occur for the same wavelengths and the slopes are similar. This reveals the presence of the same pigment composition in the upper layer, which is the first condition to assume a glaze technique.

The identification of the pigment has been done first using a spectral database made of more than 200 reference pigments and dyes [26] with a perfect plane surface. The best matches are numerically selected by the lowest least-squares distance ε between the unknown spectrum and the reference spectra, taking into account an upward translation due to the roughness of the studied surface. Figure 2 presents the four best matches corresponding to the lightest location (j) of *Mona Lisa*'s face. This comparison allows the identification of an umber pigment in the upper layer perhaps burnt and coming from Cyprus, i.e., an iron oxide with a low percentage of manganese oxide, which is in accordance with x-ray fluorescence results [20].

To check the assumption of a mixture made of vermilion and lead white, as classically used by Italian

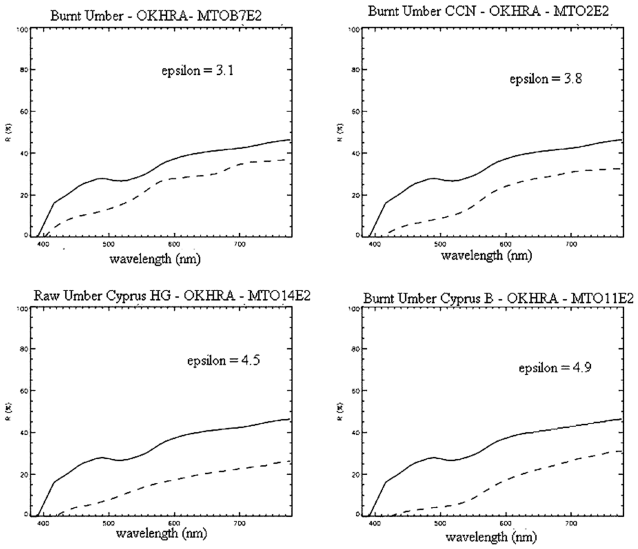

Fig. 2. Pigment identification of the upper layer corresponding to the unvarnished spectrum of location (j). The four best matches are presented with the smallest least-squares distance ε between the unknown spectrum (solid line) and those of reference pigments (dotted line) supplied by OKHRA (Provence).

painters, another spectral database made of only these mixtures with different proportions was used for the numerical comparison and did not give relevant results as shown in Fig. 3.

Finally, the recent commercial color matching software Ciba COLIBRI, developed by Ciba Konika Minolta, which can recognize pigment and pigment mixtures, was implemented and gave the same identification of an umber. The presence of a unique pigment satisfies the first criteria of a glaze technique in this upper layer.

D. Colorimetric Variations in *Mona Lisa*'s Face

The previous unvarnished spectra also allow the calculation of the trichromatic coordinates of the selected locations. The colorimetric color space CIE-Lab defined by the C.I.E. 1976 [27] has been chosen using the D65 standard illuminant (color temperature equal to 6504 K corresponding to a moderated daylight at European latitude) and the 2° standard observer defined by the C.I.E 1931. In the Cartesian representation, $L*$ is the lightness, $a*$ is the green–red axis, and $b*$ is the blue–yellow axis. In the polar representation a color is also defined by the lightness $L*$, the hue $h = \tan^{-1}(b*/a*)$, and the chroma or saturation $C = \sqrt{a*^2 + b*^2}$. The hue is essentially due to the pigment absorption property and thus presents little variation in the face due to the same pigment. The colors of the previous 11 selected areas are then presented by crosses in the plane $C*$–$L*$ in Fig. 4. This representation shows the presence of a very distinct maximum of the color saturation in the face. This maximum and the presence of a unique umber pigment are two arguments underlying the use of a glaze technique in the sfumato.

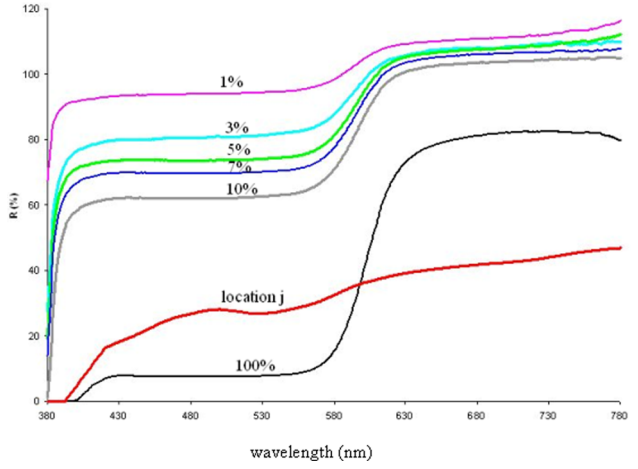

Fig. 3. (Color online) Reflectance spectra of the mixture made of vermilion and lead white with various volume concentrations in vermilion (shown above each spectrum) compared to the previous spectrum of location (j) in *Mona Lisa*'s face.

3. Modeling Using the Radiative Transfer Equation and the Auxiliary Function Method

A. Pigment Identification of the Base Layer

1. *Validity Domain of the Radiative Transfer Equation*

The radiative transfer is relevant to describe the interaction between light and scatterers if the light remains incoherent. This condition requires an incident incoherent light and a very low concentrated medium. This is the case of a glaze paint where the pigments are the scatterers illuminated by white light. Scalar variables can then be used and a flux balance is calculated with the RTE [4] for a given wavelength in a given direction defined by its angle θ with the normal to the interface or by $\mu = \cos\theta$. The flux balance is recalled in Eq. (1) for an elementary layer with an optical thickness $d\tau$:

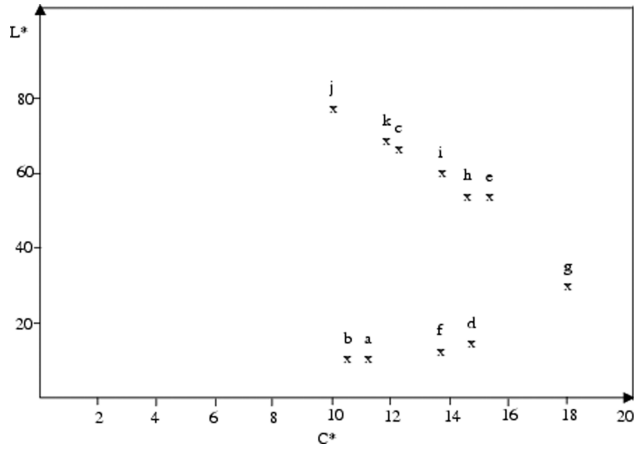

Fig. 4. Colorimetric variations in the chroma $C*$ and lightness $L*$ planes of the CIE-Lab space of *Mona Lisa*'s face deduced from the 11 previous experimental unvarnished spectra presented in Fig. 1(d).

$$\frac{dw^{\pm}(\mu,\tau)}{d\tau} = \mp\frac{w^{\pm}(\mu,\tau)}{|\mu|} \pm \frac{q}{2}[(f(\tau)+g(\tau)], \qquad (1)$$

where w^+ and w^- are the scattered flux, respectively, in the upstream and downstream directions. $\tau = \int_{x=0}^{z}(k+s)\mathrm{d}x$ is the optical thickness. The first term on the right-hand side of Eq. (1) corresponds to the attenuation of the diffuse flux due to absorption and scattering by the pigments with corresponding k and s coefficients gathered in the albedo $q = s/(k+s)$. The second term corresponds to the multiple scattering in the μ direction of the scattered flux coming from all directions μ_1 . $f(\tau)$ is the auxiliary function in the AFM and writes $f(\tau) = \int_{\mu_1=0}^{1}[w^+(\mu_1,\tau)+w^-(\mu_1,\tau)](\mathrm{d}\mu_1/\mu_1)$. The third term corresponds to the single scattering where a collimated flux W^+ coming from the μ_0 direction is scattered in the direction μ: $g(\tau) = W^+(\tau)/2\mu_o$.

The exact solving by the AFM leads to a Fredholm integral equation on $f(\tau)$ [5]. The boundary conditions for the air–glaze interfaces at $\tau = 0$ (taking into account the refractive index $n = 1.5$ of the medium) and glaze–base layer at $\tau = h$ (taking into account the reflectance factor ρ of the base layer) are then introduced. The diffuse flux coming out of the glaze layer is calculated for each wavelength and with the same configuration 57°/0° as that used for the measured spectra ($\theta = 0°$ for $\tau = 0$ and $\theta_0 = 57°$). The calculation is repeated for all the wavelengths of the visible range and the reflectance spectrum, then the corresponding trichromatic coordinates are finally deduced.

2. *Need of a Model for the Glaze Layer*

The principle of the RTE is the substitution of the real layer by an homogeneous one made of a unique kind of scatterer characterized by its absorption and scattering coefficients $k(\lambda)$ and $s(\lambda)$ and its phase function. Direct calculations of these parameters are complex for nonspherical scatterers. A model of a glaze layer is then necessary. We have previously validated such a model [1] on different glaze layers with various optical thicknesses applied on different colored base layers by comparison between measured reflectance spectra and results of the modeling. The simple model of a glaze layer with plane interfaces, isotropic scatterers, applied on a Lambertian base layer characterized by their reflectance factor $\rho(\lambda)$, is completely satisfying considering a 1% accuracy for the measurements.

3. *Optical Characteristic of the Scatterers*

The coefficients $k(\lambda)$ and $s(\lambda)$ of the previously identified burnt umber (see Fig. 2) have been deduced from two methods, both using reflectance measurements with a Cary 5 spectrometer and its integration sphere. The first one calls upon the RTE solved by the AFM for two glaze samples with different known thicknesses and the same composition. The second calls upon the two-flux method for two glaze samples with the same thickness and composition applied on a white and a black background [28]. Both methods lead to the same results, but the second one is easier to implement. The variations of $k(\lambda)$ and $s(\lambda)$ of the burnt umber are presented in Fig. 5. It must be noticed that these coefficients are proportional to the pigment volume concentration of the samples used for their determination. This remark induces that only relative optical thickness will be able to be later deduced by comparison between experimental and modeled spectra or trichromatic coordinates.

4. *Modeling for Various Optical Thickness*

The intensity of the diffuse flux calculated in the modeling will depend on the optical thickness of each layer. To implement the modeling for different optical thicknesses, we choose 13 layers made of 1–13 identical films each with a thickness equal to 5 μm and a pigment volume concentration of 2% as previously implemented [1]. These parameters are arbitrarily chosen to obtain large variations of the optical thickness and get closer to the artist's experience.

The intensity of the diffuse flux calculated in the modeling will also depend on the base layer. For this interface we choose mixtures of lead white and vermilion and the boundary condition calls upon the reflectance factor of a given mixture of lead white and vermilion (Fig. 3). The same mixture is obviously used for all 13 glaze samples. Different simulated spectra are then obtained for 1–13 glaze layers applied on the same base layer. The whole process is repeated for different concentrations of vermilion and lead white.

5. *Comparison of Simulated and Experimental Results*

The simulated reflectance spectra are in good agreement with the spectra presented in Fig. 1(d) when the reflectance factor of a red under layer made of

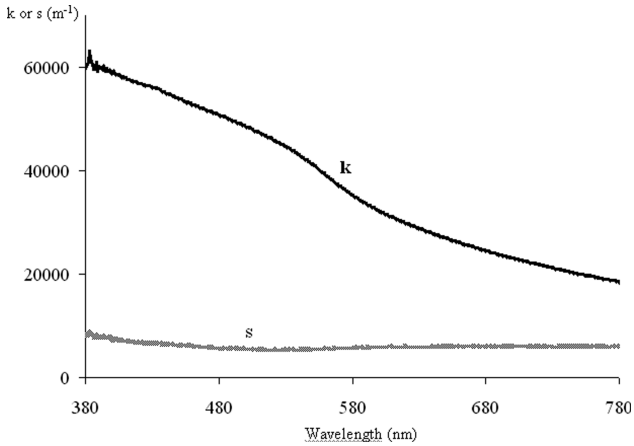

Fig. 5. Spectral variations of absorption k and scattering s coefficients (in m^{-1}) of the umber identified in the upper layer of *Mona Lisa*'s face.

1% vermilion and 99% lead white (see Fig. 3) is used, but too many simulated spectra are provided to be clearly presented on a single figure.

The simulated reflectance spectra are used to calculate the corresponding trichromatic coordinates. A spline method is then implemented for getting a curve smoothing of the results from the 13 different glaze layers applied on the same base layer. The colorimetric results deduced from this modeling are presented in Fig. 6 by a full line and are in excellent agreement with the previous results (cross) directly deduced from the unvarnished spectra. The exceptional maximum of saturation of a glaze is definitely confirmed. For other proportions of the pigment mixture of the base layer or for a lead white base layer, the simulated curves $L* = f(C*)$ never go through the experimental results. Unfortunately, it is not possible to deduce the real thickness of the glaze for the different locations (a)–(f) in *Mona Lisa*'s face because only the relative optical thickness is available from modeling related to the pigment concentration of the samples used to determine k and s, as previously noticed.

6. *Last Validations*

The extrapolation of the modeled curve for small lightness goes satisfactorily through the colorimetric coordinates of the pure umber, which corresponds to an infinite glaze layer and confirms the pigment identification of the upper layer.

The extrapolation of the curve for larger lightness, corresponding to no glaze layer, actually goes through the color of a pigment mixture of 1% vermilion and 99% lead white measured separately on a dry pigment mixture. A pure lead white, classically used for a base layer in Italy in the 16th century, has colorimetric coordinates ($L* 100$ and $C* = 0$) that do not fit with the simulated curve and thus are not satisfactory. It is the same for other mixtures of lead white and vermilion, more concentrated in red pigment, they do not lead to a relevant modeling. It

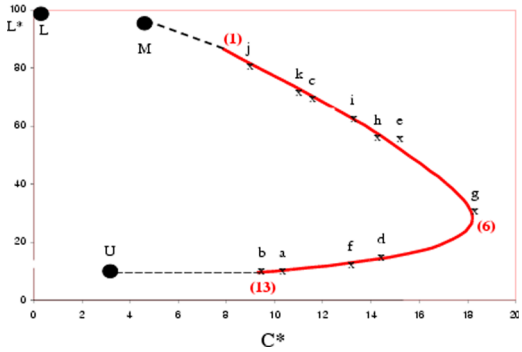

Fig. 6. (Color online) Colorimetric variations in the chroma $C*$ and lightness $L*$ planes of the CIE-Lab space, deduced from the modeling of an umber glaze (solid line) from 1–13 layers (number in parentheses) and applied on a mixture of 1% vermilion and 99% lead white. The coordinates of a pure dry lead white (L), a dry umber (U), and a dry mixture (M) of 1% vermilion and 99% lead white pigments have been added.

can then be assumed that the mixture of 1% of vermilion and 99% of lead white corresponds to the base layer on which the glaze is applied. This identification is in accordance with the detection of lead and mercury by x-ray fluorescence [20] and the present study adds the composition of the mixture and its location in the base layer.

In order to definitively exclude the case of a pigment mixture in the upper layer, we have redone the modeling for the case of an umber mixed with a lead white in various proportions. The colorimetric results are presented in Fig. 7 and, as expected, clearly show that the maximum of saturation is smaller than the one obtained with a glaze technique.

The present modeling confirms the existence of a glaze technique by the exceptional maximum of saturation. It confirms the pigment identification of the upper layer. It adds the pigment identification of the base layer. Used with a multispectral camera, the RTE solved by the AFM proves to be an innovating and powerful tool for nondestructive recognition of artistic stratified materials and techniques.

B. Explanation of the Exceptional Maximum of the Saturation

This exceptional maximum value of the saturation explains the visual appearance of such a painting with a color that seems to be built in the bulk, as opposed to the case of a pigment mixture where the color seems to come from the surface. This exceptional saturation is due to the unique kind of pigment in the glaze and can be explained by the modeling using the RTE. Its solving by the AFM allows the separation between the different contributions to the diffuse flux coming out of the paint layer. The three fluxes due to the single scattering, the multiple scattering, and the scattering by the base layer can then be separately calculated. This decomposition cannot be directly obtained by experiments, but only by the use of modeling. These calculations have already been realized for school glaze samples made of chromium oxide. We apply here the same process to *Mona Lisa*'s face and we only present the results of the

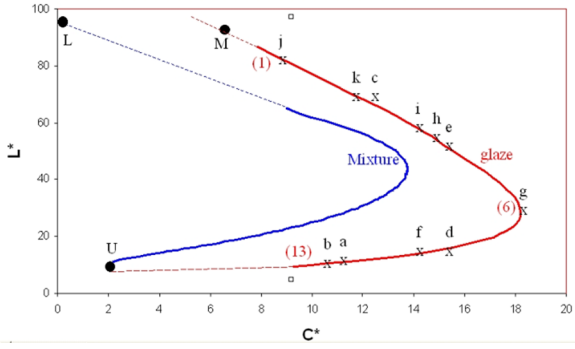

Fig. 7. (Color online) Comparison between the simulated color variations of the previous glaze and those of a pigment mixture made of umber and lead white with varying proportions .

calculations, which can be found in our previous paper [2].

The diffuse flux coming from the paint layer in the μ direction for $\tau = 0$, which is the solution of Eq. (1), can be written as the sum of three terms:

$$w^-(\mu, 0) = w^-_{ss}(\mu, 0) + w^-_{ms}(\mu, 0) + w^-_{B}(\mu, 0). \quad (2)$$

The meaning of these three terms is schematized in the second column of Fig. 8.

The first term corresponds to the light undergoing only a single scattering before coming out of the paint. The second term corresponds to the light undergoing multiple scattering before coming out of the paint. In both terms the light is only scattered by pigments and has never reached the base layer. The third term corresponds to the light scattered by the base layer. This light can undergo single or multiple scattering before or after reaching the base layer. The global flux, outcoming in the half upper hemisphere and normalized by the incident flux, is finally calculated for the three cases.

The third column of Fig. 8 presents the three global flux scattered by the 13 glaze layers made of an umber pigment applied to a mixture of 1% vermilion and 99% lead white base layer. The single scattering [see Fig. 8(a)] increases with the number of scatterers and then with the number of layers. The multiple scattering [see Fig. 8(b)] increases up to three layers and then decreases. Its variation undoubtedly underlines the origin of the maximum of saturation. Moreover, one finds again the shape of an umber spectrum. Finally, the light scattered by the base layer decreases [see Fig. 8(c)] when the number of layers increases because the base layer is less and less reached by the incident light. The shape of the spectrum corresponding to a mixture of 1% vermilion in lead white (see Fig. 3) is recognizable only for one and two glaze layers. The large values of the outcoming flux in Fig. 8(c) compared with those in Figs. 8(a) and 8(b) show that most of the light reaches the base layer according to the transparency of the glaze layers.

The corresponding colors calculated in the CIE-Lab space are presented in Fig. 9 in the $C*$–$L*$ plane. Unfortunately, the trichromatic coordinates are not additive and the sum of these three curves cannot be used to find again the global color variations presented in Fig. 6. When the light scattered by the pigments [see Figs. 8(a) and 8(b)] is completely separated from the light scattered by the base layer [see Fig. 8(c)], it is clearly shown that the maximum of the saturation is due to the multiple scattering and not to the single scattering. The last component also shows a less pronounced maximum value of the saturation once more due to the multiple scattering by pigments before and after the scattering by the base layer.

These results explain that the multiple scattering by the low concentrated pigments contained in the upper layer is the main origin of the exceptional maximum of the saturation and that the single scattering does not contribute to this maximum. This underlines the spectral filtering of each pigment, which improves with the number of interactions between light and pigment. The multiple scattering

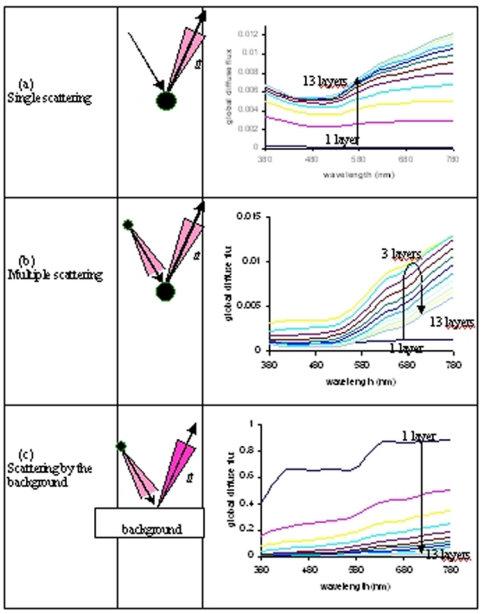

Fig. 8. (Color online) Three contributions to the global diffusion coming from the light flux, according to the number of glaze layers for an umber embedded in an oil binder and applied to a 1% vermilion and 99% lead white base layer: (a) single scattering, (b) multiple scattering, (c) scattering by the background.

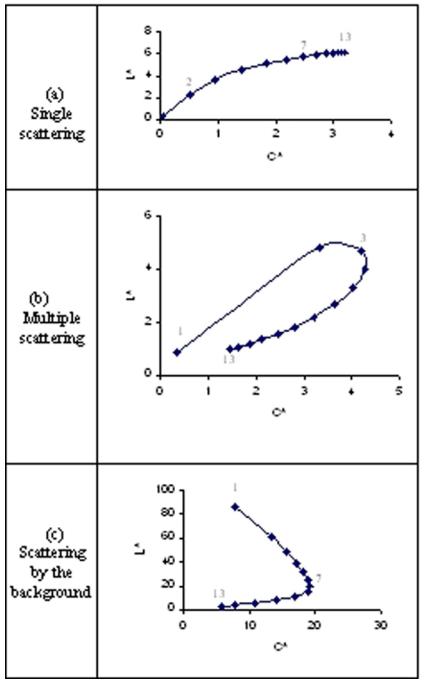

Fig. 9. (Color online) Colorimetric variations in the chroma $C*$ and lightness $L*$ planes of the CIE-Lab space as a function of the glaze layer number for each contribution to the diffuse light: (a) single scattering, (b) multiple scattering, (c) scattering by the background.

clearly favors the purity of the color, the single scattering being widely insufficient to do it. This spectral filtering by colored pigments is less effective for layers made of pigment mixtures where multiple scattering is less important due to the presence of white pigments in the medium, and this explains the smaller maximum value of the saturation in this case.

4. Conclusion

The diffuse reflectance spectra recorded by a multispectral camera after a virtual varnish removal prove that the sfumato of *Mona Lisa* is made of a single pigment with a small volume concentration, an umber, very common in Italy in the 16th century. The same spectra allow the calculation of the trichromatic coordinates in the CIE-Lab space and emphasize a large maximum value of the color saturation in the global face. These criteria attest to the use of a glaze technique inspired by the Primitive Flemish painters such as Van Eyck and Van Der Weyden, where the modulations of the color are realized by varying the number of layers without adding any white pigment. The maximum of saturation is confirmed by the modeling using the RTE solved by the AFM. The satisfactory agreement between modeling and experiments also proves that the base layer is made of a mixture of 1% vermilion and 99% lead white. Finally, the AFM explains the exceptional maximum of the saturation by separating the different origins of light scattering. The typical rendering of the sfumato is then optically explained by the predominance of the multiple scattering favored by the low concentration of one kind of pigment in a translucent medium.

Associated with a multispectral camera, the RTE solved by the AFM proved to be an innovative and powerful tool for a nondestructive recognition of artistic stratified materials and artistic techniques. Until now all the results could be obtained only by destructive sampling. In the case of *Mona Lisa*, the combination of both techniques leads to the recognition of a glaze technique and to the pigment identifications of the upper layer and the base layer. It is the first time that modeling by use of radiative transfer and the solving of the inverse problem is applied to the field of works of art, even when it is now applied in atmospheric optics, astrophysics, oceanography, and climatology. In the near future we intend to systematize the process by use of large databases of absorption and scattering coefficients of reference pigments and of reflectance spectra of classical base layers.

The previous and numerous assumptions of a glaze technique used in Leonardo's sfumato are now experimentally and theoretically attested. It remains to carry out similar studies on other Leonardo paintings such as the portrait of Cecilia Gallerani painted in 1490 (Fine Arts Museum of Cracovia) or the portrait of Ginevra de Benci painted in approximately 1479 (National Gallery of Art, Washington, D.C.) to check the presence of a sfumato before *Mona Lisa*. The results could generalize the term "sfumato" currently used to describe Leonardo's technique.

We thank Chuck Siewert, specialist of radiative transfer at the North Carolina State University; René de la Rie, head of scientific research at the National Gallery of Art, Washington, D.C.; and Yves Borensztein at Institut des Nano Sciences de Paris for their interest in the subject and their constructive proofreading of the paper.

References

1. L. Simonot and M. Elias, "Special visual effect of art glazes explained by the radiative transfer equation," Appl. Opt. **43**, 2580–2587 (2004).
2. M. Elias and L. Simonot, "Separation between the different fluxes scattered by art glazes: explanation of the special color saturation," Appl. Opt. **45**, 3163–3172 (2006).
3. E. Panofski, *Les Primitifs Flamands* (Hazan, 1992).
4. S. Chandrasekhar, *Radiative Transfer* (Dover, 1960).
5. M. Elias and G. Elias, "Radiative transfer in inhomogeneous stratified media using the auxiliary function method," J. Opt. Soc. Am. A **21**, 580–589 (2004).
6. C. N. Cochin, *Voyage Pittoresque d'Italie* (Ch.-Ant. Jombert, 1773).
7. V. Pomarède, *La Joconde* (Prat / Europa, 1988).
8. G. Vasari, *The Lives of the Artists* (Penguin, 1987), English translation.
9. J. Franck, "The Unrestorable Sfumato," in *Academia Leonardi Vinci* (UCLA , 1993), Vol. VI, p. 238.
10. M. Kemp, *Leonardo da Vinci* (Oxford, 2006).
11. D. Arasse, *Léonard de Vinci* (Hazan, 2003).
12. E. H. Gombrich, *The Story of Art* (Phaidon, 1999), p. 300.
13. K. Clark, "Mona Lisa," The Burlington Magazine **115**, 144–150 (1973).
14. M. Gelb, *The How to Think Like Leonardo Da Vinci Workbook* (Dell, 1998).
15. M. S. Livingstone, "Is it warm? Is it real? Or just low spatial frequency," Science **290**, 1299 (2000), doi: 10.1126/science .290.5495.1299b.
16. D. Queiros-Conde, "The turbulent structure of *sfumato* within *Mona Lisa*," Leonardo **37**, 223–228 (2004).
17. J. F. Asmus, "Mona Lisa symbolism uncovered by computer processing," Mater. Charact. **29**, 119–128 (1992).
18. L. L. Kontsevich and C. W. Tyler, "Making Mona frown," Science **304**, 1900 (2004), doi: 10.1126/science.304.5679 .1900b.
19. F. Blais, J. Taylor, L. Cournoyer, M. Picard, L. Borgeat, G. Godin, J. A. Beraldin, and M. Rioux, "More than a poplar plank: the shape and subtle colours of the masterpiece 'Mona Lisa' by Leonardo," Proc. SPIE **6491**, 649106 (2007).
20. J. P. Mohen, M. Menu, and B. Mottin, *Mona Lisa: Inside the Painting* (Abrams, 2006), p. 92.
21. P. Cotte and M. Dupouy, "CRISATEL: a high resolution multispectral system," Proceedings of PICS'03 Conference, Rochester, USA (2003), pp. 161–165.
22. P. Cotte and D. Dupraz, "Spectral imaging of Leonardo da Vinci's Mona Lisa: an authentic smile at 1523 dpi," Proceedings of IS&T Archiving'06, Ottawa, USA (2006), p. 228.
23. M. Elias, L. Simonot, L. M. Thoury, and J. M. Frigerio, "Bi-directional reflectance of a varnished painting part 2: influence of the refractive indices, surface state and absorption—experiments and simulations," Opt. Commun. **231**, 25–33 (2004).

24. M. Elias, M. R. De La Rie, J. Delanay, and E. Charron, "Leveling of varnishes over rough substrates," Opt. Commun. **266**, 586–591 (2006).
25. P. Cotte and D. Dupraz, "Spectral imaging of Leonardo da Vinci's Mona Lisa: a true colour smile without the influence of aged varnish," Proceeding IS&T CGVI '06, **311**, Leeds, UK (2006).
26. G. Dupuis, M. Elias, and L. Simonot, "Pigment identification by fiber-optics diffuse reflectance spectroscopy," Appl. Spectrosc. **56**, 1329–1336 (2002).
27. G. Wyszecki and W. S. Stiles, *Color Science: Concepts and Methods, Quantitative Data and Formulae* 2nd ed. (Wiley, 1982).
28. G. Latour, M. Elias, and J. M. Frigerio, "Color modeling of stratified pictorial layers using the radiative transfer equation solved by the auxiliary function method," J. Opt. Soc. Am. A **24**, 3045–3053 (2007).